

Cavitands as Reaction Vessels and Blocking Groups for Selective Reactions in Water

Daniele Masseroni, Simone Mosca, Matthew P. Mower, Donna G. Blackmond,* and Julius Rebek, Jr.*

Abstract: The majority of reactions currently performed in the chemical industry take place in organic solvents, compounds that are generally derived from petrochemicals. To promote chemical processes in water, we examined the use of synthetic, deep water-soluble cavitands in the Staudinger reduction of long-chain aliphatic diazides (C_8 , C_{10} , and C_{12}). The diazide substrates are taken up by the cavitand in D_2O in folded, dynamic conformations. The reduction of one azide group to an amine gives a complex in which the substrate is fixed in an unsymmetrical conformation, with the amine terminal exposed and the azide terminal deep and inaccessible within the cavitand. Accordingly, the reduction of the second azide group is inhibited, even with excess phosphine, and good yields of the monofunctionalized products are obtained. In contrast, the reduction of the free diazides in bulk solution yields diamine products.

We recently developed new container molecules—deep, water-soluble cavitands **1** (Figure 1) that function over a large pH range—as vessels for reagents reluctant to enter water.^[1] The containers are vase-shaped structures that use the principles of molecular recognition to target molecules of complementary sizes, shapes, and chemical surfaces. The key to their function as receptors in water is the burial of hydrophobic guests within the cavitand host. We demonstrate here the advantages of folded guest shapes within cavitands to dramatically alter the reactivities of two ends of a symmetrical substrate. These molecular containers offer access to reaction selectivities that are unknown in bulk solution. Specifically, we applied the Staudinger reaction^[2] (Scheme 1) to reduce

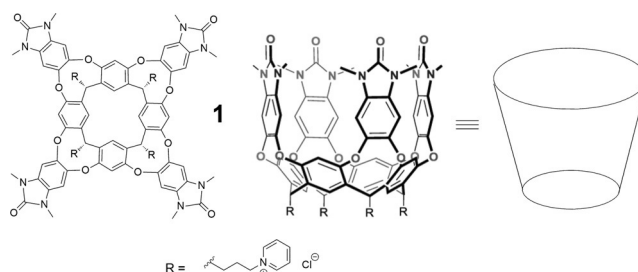
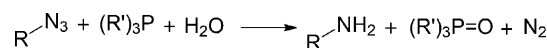


Figure 1. Chemical formula, conformation, and schematic representation of the deep, water-soluble cavitand **1**.



Scheme 1. Staudinger reduction.

α,ω -diazides to monoamines within **1** by using trimethylphosphine (PMe_3) in D_2O . The reaction of azides and triaryl- or trialkylphosphines reliably forms amines almost quantitatively under mild conditions through iminophosphorane intermediates.^[3] If the reaction is performed in aqueous solvent, the iminophosphorane intermediates are readily hydrolyzed to yield the primary amines and phosphine(V) oxide. In our study, the differences in the folding conformations of the starting materials and the desired products within the cavitand gave rise to exceptional product distributions.

Sonication of α,ω -diazides with **1** gave stoichiometric host–guest complexes, with their 1H NMR spectra showing characteristic upfield-shifted signals (Figure 2; see also the Supporting Information). There are well-established experimental and computational correlations between upfield shifts and positions of nuclei within this and related cavitands.^[1] The eight aromatic panels of the container create a magnetic anisotropy that shields nuclei from the applied magnetic field of the spectrometer. Nuclei in the deepest parts of the cavitand experience the largest upfield shifts ($\Delta\delta$ of -4 to -5 ppm) and those near the rim the smallest upfield shifts ($\Delta\delta$ of -0.5 to 0 ppm). However, the diazides show signals clustered around 0 to -1.3 ppm (i.e. $\Delta\delta$ of -1 to -2 ppm). Accordingly, the methylene groups are not fixed at the top or at the bottom of the cavity. Instead, they are in a rapid, dynamic equilibrium, whereby a given methylene group resides sometimes deep inside the cavitand (where it experiences a $\Delta\delta$ of -4 ppm) and sometimes outside (where no shift occurs). A symmetrical compound must spend equal times in the two environments, so the average $\Delta\delta$ value of the magnetic environments is about -2 ppm. This places the signals for the nondescript methylene groups at around

[*] Dr. D. Masseroni, Prof. Dr. J. Rebek, Jr.
Department of Chemistry, Fudan University
220 Handan Road, Shanghai 200433 (China)

Dr. S. Mosca
Department of Biotechnology and Biosciences
University of Milano-Bicocca
20126 Milano (Italy)

Dr. S. Mosca, M. P. Mower, Prof. Dr. D. G. Blackmond,
Prof. Dr. J. Rebek, Jr.
Department of Chemistry and The Skaggs Institute for Chemical
Biology, The Scripps Research Institute
10550 North Torrey Pines Road, La Jolla, CA 92037 (USA)
E-mail: blackmond@scripps.edu
jrebek@scripps.edu

Supporting information (synthesis and characterization of new compounds, materials, methods for all experiments, kinetic modeling details, and additional spectral data) and the ORCID identification number(s) for the author(s) of this article can be found under <http://dx.doi.org/10.1002/anie.201602355>.

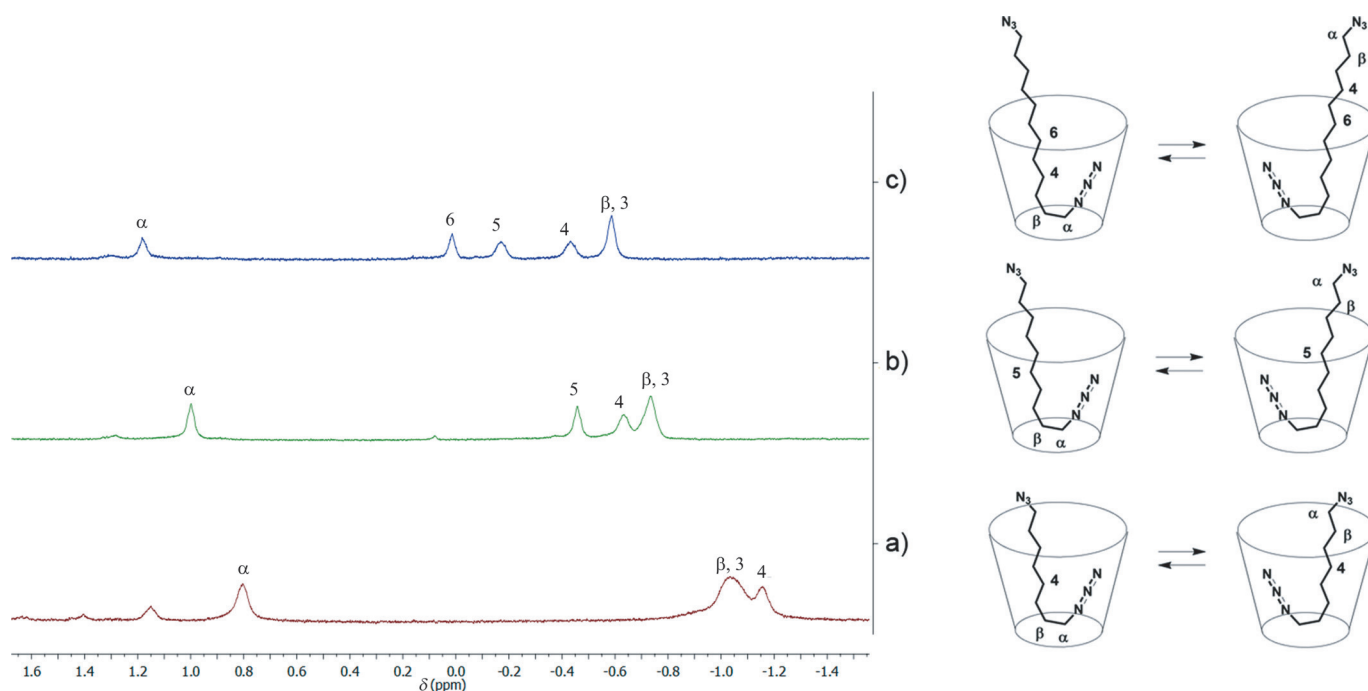


Figure 2. Left: Upfield portions of the ^1H NMR spectra of α,ω -diazide@cavitand 1 complexes (400 MHz, 298 K, D_2O): a) (diazide C_8)@cavitand; b) (diazide C_{10})@cavitand; c) (diazide C_{12})@cavitand. Right: Schematic representations of diazide C_8 , C_{10} and C_{12} in the cavitand as the rapidly interconverting J-shaped conformations of the guest.

−0.7 ppm, where they in fact appear. The ^1H NMR spectra of the diazides indicate time-averaged and unsymmetrical J-shaped arrangements rather than fixed and symmetrical, U-shaped ones. The situation is depicted in Figure 2 (see also the Supporting Information). Attempts to freeze out the motion at lowered temperatures were unsuccessful.

Treatment of the complexes in D_2O with an excess of PMe_3 (3 equivalents) in an NMR tube induces changes in the spectra. Figure 3 shows, as an example, the changes for the complex of C_{12} (for C_{10} and C_8 , see the Supporting Information). Dimethylsulfoxone^[4] was used as an internal standard, and the product distribution with time is shown in the stacked spectra. The new resonances that appear match the signals of authentic monoamine monoazide C_{12} inside the cavitand (see the Supporting Information).

The methylene signals of both the monoamine and diamine in the cavitand appear further upfield than those of the diazide, and are consistent with static complexes. The assignments shown in Figure 3 are based on COSY spectra (see the Supporting Information) and reflect the correlation of the upfield shift ($-\Delta\delta$) with the depth of the nuclei in the cavity. The diamine shows the typical upfield shifts of a conventionally folded bola-amphiphile.^[1] Most informatively, the methylene groups α and β to the monoazide are shifted furthest upfield. The steric requirements of the narrow N_3 function apparently allow a sharp bend in its attached chain that can penetrate deeply into the cavitand. The fixed conformation of this complex buries the azide end inside the cavity, thereby isolating it from the bulk solution and preventing reaction with PMe_3 . The addition of another three equivalents of phosphine to the reaction mixture after

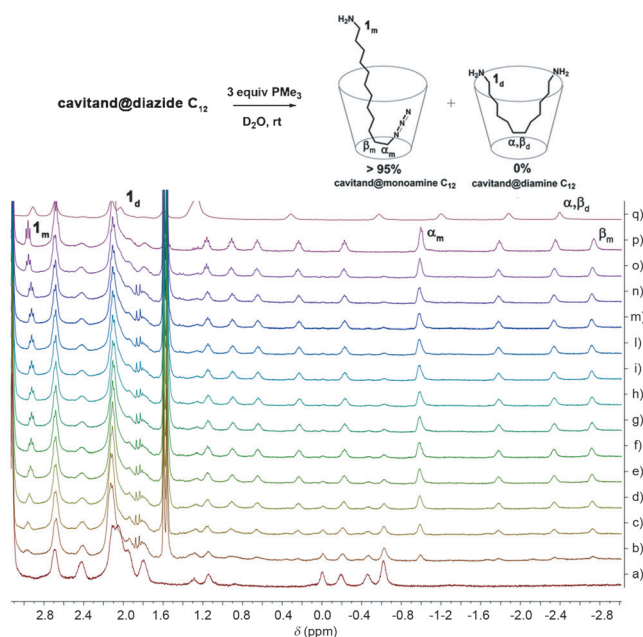


Figure 3. Top: Illustration of the Staudinger reduction of the (diazide C_{12})@cavitand complex in D_2O , with suggested conformations of the possible products inside the container. Bottom: Partial NMR spectra of the reduction reaction of diazide C_{12} (exp. $\text{C}_{12(a)}$; see the Supporting Information) chaperoned by cavitand 1 (400 MHz, 298 K, D_2O): a) diazide C_{12} complex in D_2O ; b) addition of 3 equiv of PMe_3 to (a), 15 min; c) 30 min; d) 45 min; e) 60 min; f) 75 min; g) 90 min; h) 105 min; i) 120 min; j) 135 min; m) 150 min; n) 210 min; o) 25 h; p) authentic C_{12} monoamine monoazide in cavitand 1 in D_2O ; q) authentic C_{12} diamine in cavitand 1 in D_2O .

24 h (or to the authentic monoazide complex for control, see the Supporting Information) did not change the chemical shifts or the integrals of the spectra, thus confirming that the remaining azide group is inaccessible to the reducing agent. The striking ability of the cavitand to suppress the rapid interconversion of the two ends of the molecule in and out of the cavitand once one azide has been reduced to an amine rationalizes the excellent selectivity afforded by the chapter-one.

Figure 4 shows the kinetic profile of the reaction of the C_{12} diazide within cavitand, taken from integration of the NMR time course data in Figure 3. Rapid consumption of the diazide to form an intermediate species suggested to be an iminophosphorane is followed by quantitative conversion into the monoamine product in less than three hours, with no formation of the diamine product observed.

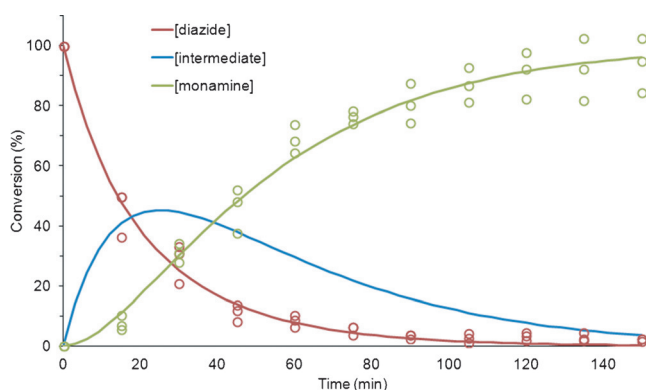
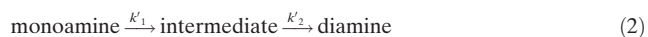


Figure 4. Product distribution and kinetic model curves for the reduction of diazide C_{12} with cavitand **1**. Open circles represent experimental data from three runs; lines represent the kinetic model of Equations (1) and (2).^[5]

The sequential reaction can be modeled from the experimental data according to Equations (1) and (2). Formation of an intermediate (rate constant k_1) precedes its hydrolysis (rate constant k_2) to the monoamine product. A second sequential reaction converting the monoamine into the diamine product (with k_1' and k_2') occurs only in the absence of the cavitand.



The function of the cavitand may be thought of as a loosely held blocking group: once the first reduction step occurs, the cavitand suppresses the rapid equilibration of the two ends of the molecules, thus hiding the second azide site and thereby altering the reaction product selectivity. The formation and build up of the intermediate iminophosphorane is not directly observed due to interference from other signals in the NMR spectra of complex **I** under the reaction conditions. However, the observation of signals attributed to the iminophosphorane in the solution reaction (see the Supporting Information) and consideration of literature

reports of this reaction supports this assignment for complex **I**. Build up of this intermediate may be responsible for the poor material balance based solely on diazide and monoamine during the early part of the reaction. As shown in Figure 4, the kinetic model based on Equations (1) and (2) provides a good fit to the temporal concentration data for the substrate and product, thus allowing an estimate of the temporal concentration of the presumed iminophosphorane intermediate.^[5]

Similar results were obtained with the C_{10} diazide; nearly quantitative yields were observed for the monoamine. An accurate determination of the distribution of the molecular species was not possible with the shorter diazide (C_8). The resonances of the guests became broadened after addition of the phosphine. Nevertheless, integration of the monoamine signals in the NMR spectrum after 24 h reaction gave a rough estimate, with the yield around 50–60 % (see the Supporting Information). The deeper complex formed by the C_8 diazide (Figure 2) compared to C_{10} or C_{12} diazides could explain its lowered reactivity toward PMe_3 in solution.

Control experiments (without cavitand) were performed both with diazides using $[\text{D}_8]2$ -propanol as cosolvent and with the monoreduced azide in D_2O . The reaction outcomes were monitored by ^1H NMR spectroscopy (the Supporting Information). In the absence of the cavitand, diazides and monoaminoazides are both converted quantitatively into the diamines, without any traces of the monoamine product, again highlighting the striking ability of the cavitand to suppress the second reduction step.

Table 1 summarizes the rate constants determined from kinetic modeling studies of the reactions using COPASI software^[5] with and without cavitand. Comparison of the values of k_1 to k_1' and k_2 to k_2' supports the hypothesis that the kinetics of the sequential reaction of azide to amine is similar with and without the cavitand, and the primary role of the cavitand is to suppress the onward reaction of the monoamine to the diamine product.

Table 1: Rate constants derived from kinetic modeling of the sequential reactions according to Equations (1) and (2).^[a]

Substrate	Diazide with cavitand $k_1^{[b]}$	$k_2^{[b]}$	Monoamine without cavitand $k_1'^{[b]}$	$k_2'^{[b]}$
C_{12}	36.4	0.026	30.4	0.032
C_{10}	26.6	0.029	13.4	0.044
C_8	— ^[c]	— ^[c]	13.1	0.045

[a] Modeling studies carried out using COPASI software.^[5] [b] Units of rate constants are $\text{M}^{-1} \text{h}^{-1}$. [c] k_1 and k_2 for diazide C_8 with cavitand could not be calculated because of inaccurate integration measurements of the NMR spectrum.

A variety of contorted alkane shapes are observed in closed systems such as capsules^[6] and open-ended systems such as cyclodextrins^[7] and cucurbiturils.^[8] In earlier studies, we used the folded conformations that bring the guest ends close together to promote macrolactamization reactions in cavitands.^[9] Here, the cavitand plays a complementary and contrasting role by inhibiting the further reactions of a folded guest; this overcomes a general problem of the monofunc-

tionalization of symmetrical compounds.^[10] When the two reaction sites on a molecule are remote such that they act independently, statistically determined yields are obtained; the yield of the desired monofunctionalized product under these circumstances is <50%, a common bane of such reactions.

The cavitand plays two roles in the reactions in this study: first, it acts as a vehicle that facilitates reactions in water, and second, it behaves as a supramolecular protecting group^[11] in which the mechanical barriers of the walls isolate reactive functions from reagents in solution. The unprecedented effect on the chemical selectivity of the present monofunctionalization reaction requires use of the cavitand as a stoichiometric agent to chaperone each substrate molecule. However, the cavitand can be recovered by simple extraction for use in further reactions (see the Supporting Information), and we are working toward combining these processes toward the goal of true catalysis with turnover.

Acknowledgements

This research was supported by the Thousand Talents Program, Fudan University of Shanghai, China, the National Science Foundation of the USA (CHE 1506266), and a Marie Curie International Outgoing Fellowship within the 7th European Community Framework Programme; Grant PIOF-GA-2013-627403 provided a postdoctoral fellowship (to S.M.).

Keywords: cavitands · diazides · selectivity · Staudinger reduction · supramolecular chemistry

How to cite: *Angew. Chem. Int. Ed.* **2016**, 55, 8290–8293
Angew. Chem. **2016**, 128, 8430–8433

- [1] K.-D. Zhang, D. Ajami, J. V. Gavette, J. Rebek, Jr., *J. Am. Chem. Soc.* **2014**, 136, 5264–5266.
- [2] H. Staudinger, J. Meyer, *Helv. Chim. Acta* **1919**, 2, 635–646.
- [3] a) M. Köhn, R. Breinbauer, *Angew. Chem. Int. Ed.* **2004**, 43, 3106–3116; *Angew. Chem.* **2004**, 116, 3168–3178; b) Y. G. Gololobov, L. F. Kasukhin, *Tetrahedron* **1992**, 48, 1353–1406.
- [4] G. F. Pauli, B. U. Jaki, D. C. Lankin, *J. Nat. Prod.* **2005**, 68, 133–149.
- [5] S. Hoops, S. Sahle, R. Gauges, C. Lee, J. Pahle, N. Simus, M. Singhal, L. Xu, P. Mendes, U. Kummer, *Bioinformatics* **2006**, 22, 3067–3074.
- [6] S. Liu, D. H. Russell, N. F. Zinnel, B. C. Gibb, *J. Am. Chem. Soc.* **2013**, 135, 4314–4324.
- [7] N. J. Turro, T. Okubo, C.-J. Chung, *J. Am. Chem. Soc.* **1982**, 104, 1789–1794.
- [8] K. Baek, Y. Kim, H. Kim, M. Yoon, I. Hwang, Y. H. Ko, K. Kim, *Chem. Commun.* **2010**, 46, 4091–4093.
- [9] S. Mosca, Y. Yu, J. V. Gavette, J. Rebek, Jr., *J. Am. Chem. Soc.* **2015**, 137, 14582–14585.
- [10] F. Z. Dorwald in *Side Reactions in Organic Synthesis: A Guide to Successful Synthesis Design*, Wiley-VCH, Weinheim, **2005**, pp. 333–348.
- [11] See, for examples: a) E. Elacqua, P. Kaushik, R. H. Groeneman, J. C. Sumrak, D.-K. Bucar, L. R. MacGillivray, *Angew. Chem. Int. Ed.* **2012**, 51, 1037–1041; *Angew. Chem.* **2012**, 124, 1061–1065; b) R. M. Yebeutcho, E. Dalcanele, *J. Am. Chem. Soc.* **2009**, 131, 2452–2453; c) H. Ren, Z. Huang, H. Yang, H. Xu, X. Zhang, *ChemPhysChem* **2015**, 16, 523–527; d) B. Breiner, J. K. Clegg, J. R. Nitschke, *Chem. Sci.* **2011**, 2, 51–56; e) M. M. J. Smulders, J. R. Nitschke, *Chem. Sci.* **2012**, 3, 785–788.

Received: March 7, 2016
Published online: June 2, 2016